Revista Mexicana de Astronomía y Astrofísica, **53**, 45–52 (2017)

LIMITS TO THE MAGNETIC FIELD IN THE PLANETARY NEBULA NGC 246 FROM FARADAY ROTATION

L. F. Rodríguez,[1] C. Carrasco-González,[1] J. Cantó,[2] A. Pasetto,[3] A. C. Raga,[4] and D. Tafoya[1]

Received August 4 2016; accepted September 29 2016

RESUMEN

Presentamos observaciones de radiocontinuo de la fuente extragaláctica linealmente polarizada J0047−1150, cuya línea de visión atraviesa a la nebulosa planetaria galáctica NGC 246. Determinamos el ángulo de posición del vector eléctrico para siete frecuencias entre 1.3 y 1.8 GHz, sin encontrar evidencia de rotación de Faraday y obtenemos un límite superior a 4-σ de 9.6 rad m^{-2} para la medida de rotación, lo cual implica un límite superior de 1.3 μG para el valor promedio del campo magnético en la línea de visión. Sin embargo, demostramos que la medida de rotación a lo largo de una fuente con campo magnético de morfología dipolar prácticamente se cancela. Entonces, si el campo magético tiene esta morfología, los valores locales del campo magnético en NGC 246 pueden ser mucho mayores y no se harían evidentes en un experimento de rotación de Faraday.

ABSTRACT

We present radio continuum observations of the linearly polarized extragalactic source J0047−1150, whose line of sight traverses the galactic planetary nebula NGC 246. We determine the position angle of the electric vector at seven frequencies between 1.3 and 1.8 GHz, finding no evidence of Faraday rotation and setting a 4-σ upper limit to the rotation measure of 9.6 rad m^{-2}, which implies an upper limit to the average line-of-sight component of the magnetic field in NGC 246 of 1.3 μG. However, we show that the rotation measure across a source with a dipolar magnetic field morphology practically cancels out. Therefore, if the magnetic field has this morphology, the local values of the magnetic field in NGC 246 could be much larger and will not be evident in a Faraday rotation experiment.

Key Words: ISM: magnetic fields — planetary nebulae: individual (NGC 246) — plasmas — polarization

1. INTRODUCTION

Magnetic fields are a key component in the understanding of the origin and evolution of astrophysical objects. From theoretical and observational studies we know that in the Universe there are magnetic fields going from values in the range of 10^{-17} to 10^{-14} G in the intergalactic medium (Essey et al. 2011) to values as high as 10^{15} G in some magnetars (Tiengo et al. 2013).

A variety of techniques has been used to estimate these magnetic fields. In the case of diffuse galactic regions of ionized gas, namely HII regions and planetary nebulae, there are only a handful of measurements. For HII regions, the technique of Faraday rotation has provided values in the range of about 1 to 40 μG for a few sources (Heiles & Chu 1980; Heiles et al. 1981; Harvey-Smith et al. 2011; Rodríguez et al. 2012; Purcell et al. 2015; Costa et al. 2015). The search for the Zeeman effect in radio recombination lines from the ionized gas in HII regions has set upper limits of a few (Troland & Heiles 1977) to a few tens of mGauss (mG; Roberts et al. 1991). To our knowledge, the only detection of the Zeeman effect in hydrogen radio recombination lines is that of the H30α emission from the photoevaporating disk of the Be star MWC 349 (Thum & Morris 1999). An average strength of 22 mG was derived from these observations. This discussion indicates

[1]Instituto de Radioastronomía y Astrofísica, UNAM, México.
[2]Instituto de Astronomía, UNAM, México.
[3]Max-Planck Institut für Radioastronomie, Germany.
[4]Instituto de Ciencias Nucleares, UNAM, México.

that the Faraday rotation technique is much more sensitive than the Zeeman technique. However, it requires the fortuitous circumstance of the studied source being located in front of a relatively bright, linearly polarized source, typically a quasar. The Faraday rotation is the rotation of the electric vector position angle (EVPA) of the linearly polarized emission that occurs when an electromagnetic wave passes through a magnetized medium. It is described by the value of the rotation measure (RM), that contains information about two important elements of the intervening medium: the electron density and the strength of the component of the magnetic field parallel to the line of sight.

A planetary nebulae (PN) is an ionized shell of gas around an evolved low mass star that is on its way to becoming a white dwarf. Planetary nebulae are classic objects of astrophysical study, and parameters such as the electron density and temperature, as well as the chemical composition are well known. However, similarly to many astronomical objects, there are no reliable measurements of their magnetic fields. Magnetic fields have been determined for the central stars of a handful of PNe, with values in the range of hundreds to thousands of Gauss (Jordan et al. 2005; Steffen et al. 2014). Also, from observations of the Zeeman effect in OH and H_2O masers, magnetic fields have been estimated to be in the order of mG to tens of mG in the dense, molecular structures found surrounding protoplanetary nebulae and young planetary nebulae (e. g. Hu et al. 1993; Trigilio et al. 1998; Miranda et al. 2001; Vlemmings & van Langevelde 2008; Leal-Ferreira et al. 2013; Qiao et al. 2016). More recently, the linearly polarized dust emission observed in the envelopes of protoplanetary nebulae has been proposed as a tool to estimate the magnetic field in these environments (Sabin et al. 2014).

However, there are no measurements for the ionized envelope that characterizes classical PNe (with electron densities in the range of $10^2 - 10^4$ cm^{-3}), although Ransom et al. (2010a, 2010b; 2015) have recently reported magnetic field estimates for a few old, diffuse, PNe that turn out to be similar to those of the interstellar medium. From the previous range of magnetic fields and taking into account that the average magnetic field in the diffuse interstellar medium is $\approx$5 μG (Cox 2005), we can crudely "interpolate" that a magnetic field of the order of $\approx$10-100 μG is expected for the ionized shell that forms the classical PNe. Another estimate can be made considering the fact that in the average Galactic interstellar medium (of density $n \approx 1$ cm^{-3}) the magnetic field has a value of $\approx 5\,\mu$G (Cox 2005) and using the $B \propto n^{1/2}$ scaling proposed by Fleck (1983) we obtain an estimate of $\approx 50 \rightarrow 500$ μG for the ionized shell of a classical PNe.

In this paper we present radio observations toward the PN NGC 246. This PN has an angular extent of $\approx 4'$, and was found by us to have an extragalactic source behind it. In § 2 we describe the nebula in more detail as well as the observations. In § 3 we report our results and discuss the implications for magnetic fields in PNe. Finally, we present our conclusions in § 4.

2. SEARCH FOR SOURCES AND OBSERVATIONS

We searched for planetary nebulae with a background extragalactic source that could be used to measure the Faraday rotation by analyzing images from the NRAO Very Large Array (VLA) Sky Survey (NVSS; Condon et al. 1998). Finding background objects in the solid angle of the relatively compact planetary nebulae is difficult, given the modest angular resolution of the NVSS (45″). However, in the case of extended ($> 1'$) planetary nebulae we were successful in finding one planetary nebula, NGC 246, that appeared to have a background source. To verify the presence of the compact source we obtained images of NGC 246 (using VLA archive data from project AP110, taken at 20 cm in the D configuration in 1986 January 5), both with all the *(u,v)* data and also removing the short spacings (below 1 kλ), so as to suppress the extended emission with angular dimensions above $\approx 3'$. In Figure 1 we show the radio images of NGC 246, where it is apparent that when the extended radio emission is suppressed, we clearly see the compact background source. We checked that this compact emission was not due to an ionized knot in the nebula by a comparison with the red image of the Digital Sky Survey (DSS) that does not show increased emission at the position of the radio source (see Figure 1). These data did not have the sensitivity to search for Faraday rotation and we requested time in the JVLA for an *ad hoc* observation.

The new observations were made with the Karl G. Jansky Very Large Array (JVLA) on 2014 January 20 at L band. On that date, the JVLA was in its B configuration providing an angular resolution of 4.″3. We observed continuum emission in the frequency range from 1 to 2 GHz. The total bandwidth was divided in 16 spectral windows with 64 channels of 1 MHz each. Nine out of the 16 spectral windows were not used due to strong RFI. Flux and

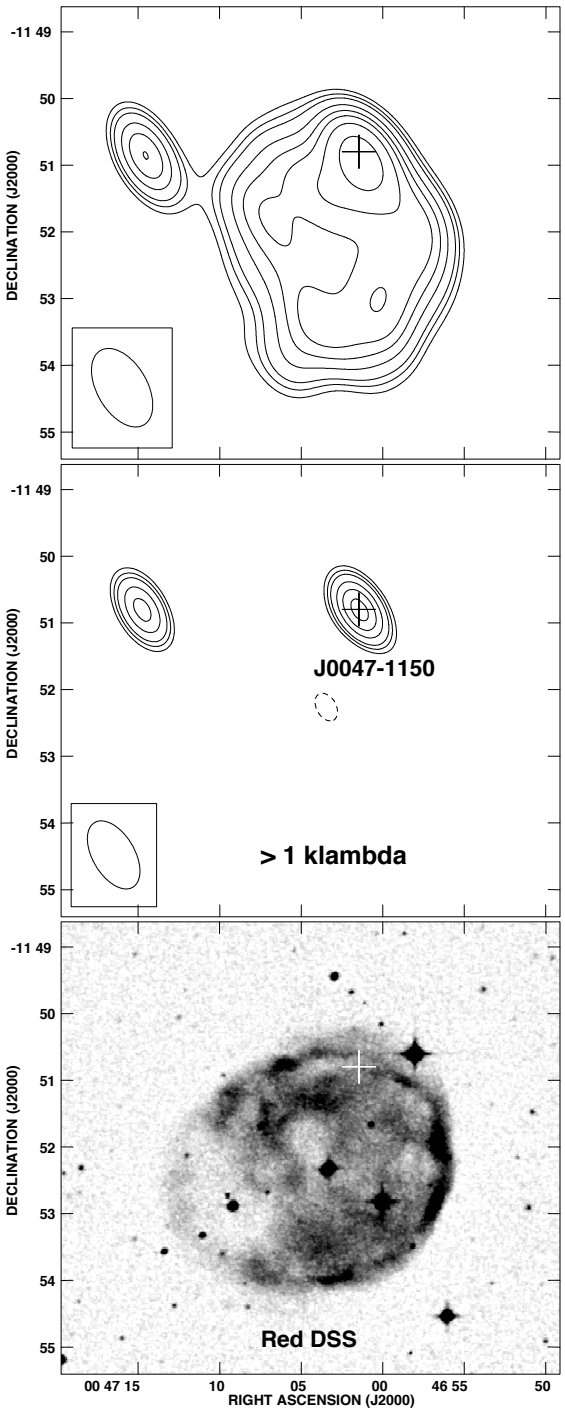

Fig. 1. (Top) Archive 20-cm VLA image of NGC 246. The cross marks the position of the proposed background source. Contours are -4, 4, 5, 6, 8, 10, 12, 15 and 20 times 1 mJy beam^{-1}. The beam is shown in the bottom left corner. (Middle) Same as above but with the short spacing visibilities ($\leq$ 1 kλ) not used. The extended emission of the PN is suppressed and we only detect two compact sources. The source to the west is J0047−1150 and the source to the east is, most probably, another extragalactic source. This last source does not have detectable linear polarization and its rotation measure could not be determined. (Bottom) Red image from the DSS. The lack of enhanced optical emission at the position of the compact radio source indicates that it is not associated with the nebula.

gain calibrations were performed by observing 3C48 and J0110−0741, respectively. For the flux calibrator, we used a resolved model of the Stokes I parameter. The polarization angles were calibrated by assuming a model for the Stokes Q and U parameters on 3C48 according to the known values of polarization angle and polarization degree from Perley and Butler (2013). The leakage of crosstalk polarization components between feeds was calibrated through an observation of 3C84, which is a well known unpolarized quasar. We followed standard procedures for the Stokes I and Stokes Q and U parameter calibration of the data by using the reduction package Common Astronomy Software Applications (CASA). Images of the Stokes I, Q and U parameters for each 64 MHz spectral window were made with the task clean of CASA.

3. RESULTS AND INTERPRETATION

In Figure 2 we show the position angle of the electric vector as a function of λ^2 for two sources: J0110−0741 and J0047−1150. The J0110−0741 source ($\alpha(J2000) = 01^h\ 10^m\ 50.0210^s$; $\delta(J2000) = -07^\circ\ 41'\ 41.114''$) is the one used in our observations as gain calibrator (see above). It clearly shows a significant rotation measure, RM=+195.0±3.7 rad m^{-2}. This source is not included in the 37,543 sources of the NVSS Rotation Measures Catalogue (Taylor et al. 2009). Analyzing this database, we find that 1.6% of the sources have rotation measures with an absolute value of 195 rad m^{-2} or more. We conclude that the rotation measure of J0110−0741 is somewhat large, but not unusual.

In contrast, the J0047−1150 source ($\alpha(J2000) = 00^h\ 47^m\ 01.382^s$; $\delta(J2000) = -11^\circ\ 50'\ 49.61''$; see Figures 1 and 2) shows no detectable rotation measure with a 4-σ upper limit of 9.6 rad m^{-2}. Again, analyzing the database of Taylor et al. (2009), we find that 26% of the sources have rotation measures with an absolute value ≤9.6 rad m^{-2}. We conclude that the rotation measure of J0047−1150 is on the small side, but is not atypical. Recently, Farnes et al. (2014) presented a catalog of multi-wavelength linear polarization and total intensity radio data for polarized sources from the NVSS. The result of this work is a catalog of 951 sources with spectral energy distributions in both total intensity and fractional polarization. The RM distribution of these objects is very similar to that of the Taylor et al. (2009) database.

We therefore ask: why is there no detectable rotation measure in J0047−1150? One possibility is that there are significant magnetic fields associated with the quasar and with the PN, but with different signs, so that they happen to nearly cancel out. Depolarization within the cloud could be another cause. If the medium is inhomogeneous or several different regimes are present within the beam, the RM can change within the source, and a deviation, more or less strong, from the classic λ^2 law

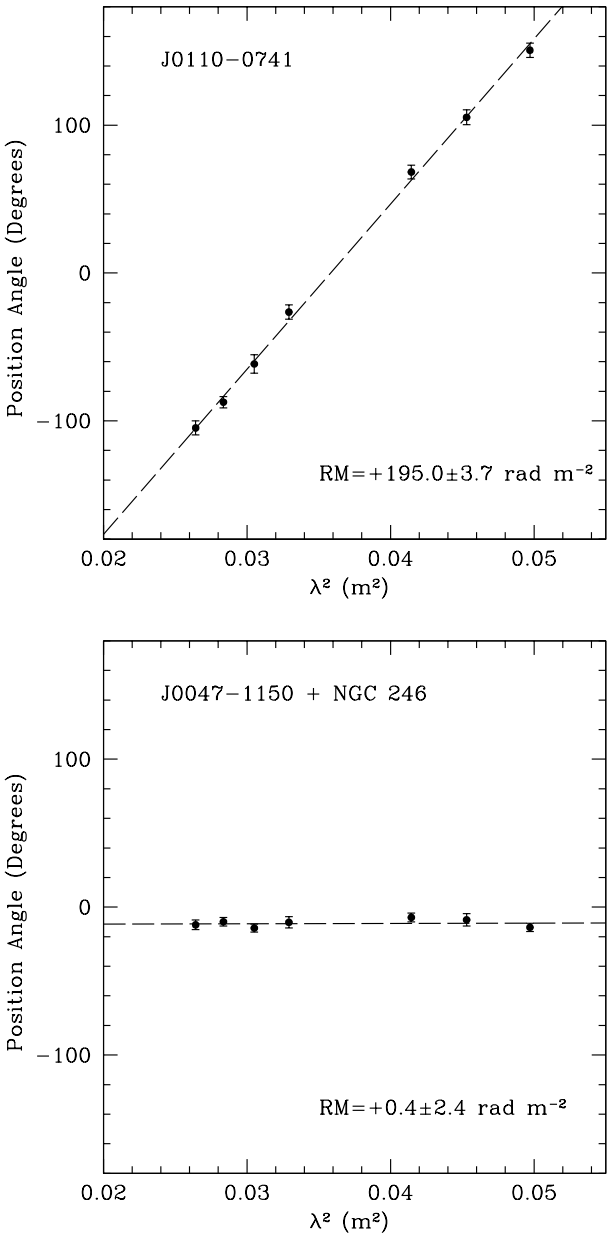

Fig. 2. (Top) Position angle of the electric vector as function of λ^2 for the gain calibrator J0110−0741. (Bottom) Position angle of the electric vector as function of λ^2 for the background source J0047−1150, whose line of sight goes through NGC 246.

can take place (Burn 1966; Vallee 1980; Saikia & Salter 1988). When this is the case, a reduction of the fractional polarization (a depolarization) is also expected. However, the linear polarization of J0047−1150 is practically constant, smoothly changing from 11.9% to 14.9% across the wavelength range shown in Figure 2.

We will explore the possibility that the quasar itself (J0047−1150) has little rotation measure and that the radiation does not experience significant Faraday rotation in going through NGC 246. This allows us to set an upper limit to the average magnetic field of NGC 246 parallel to the line of sight.

From the data shown in Figure 1, we find that the peak flux density of the nebular emission in the direction of J0047−1150 has a value of ≈11.2 mJy beam^{-1} for a beam with dimensions $73\farcs9\times43\farcs6$; $PA = 28.8°$. At a frequency of 1.49 GHz this flux density corresponds to a brightness temperature of ≈1.9 K. Assuming an average electron temperature of 2.0×10^4 K (Muthu et al. 2000), we estimate a free-free opacity of ≈0.0001 and an emission measure of 340 cm^{-6} pc. Adopting a distance of 495 pc for NGC 246 (Bond & Ciardullo 1999) and assuming that the physical depth in the line of sight is comparable to the projected chord at the position of the background source, we obtain a physical depth of 0.22 pc.

Also assuming that the nebula is homogeneous, we derive an average electron density of ≈40 cm^{-3}. This value is in agreement with estimates from optical observations (Hua et al. 1998). With these parameters and using the usual formulation for Faraday rotation (e.g. Rodríguez et al. 2012), we set a 4-σ upper limit to the average magnetic field component parallel to the line of sight of $B_\parallel \leq 1.3$ μG. This is a very low value for the magnetic field, lower even than the typical value for the diffuse interstellar medium, ≈5 μG (Cox 2005). Given the uncertainties of the measurement, we cannot rule out the possibility that the nebula has a magnetic field comparable to that of the diffuse interstellar medium.

One possible way out of this situation is to argue that the local values of the magnetic field are much larger but that some property of the planetary nebula cancels the contributions along the line of sight. In particular, in the next section we show that, interestingly, the rotation measure across a magnetic field with dipolar morphology practically cancels out and could explain our results even if the absolute values of the magnetic field in NGC 246 are much larger than our upper limit.

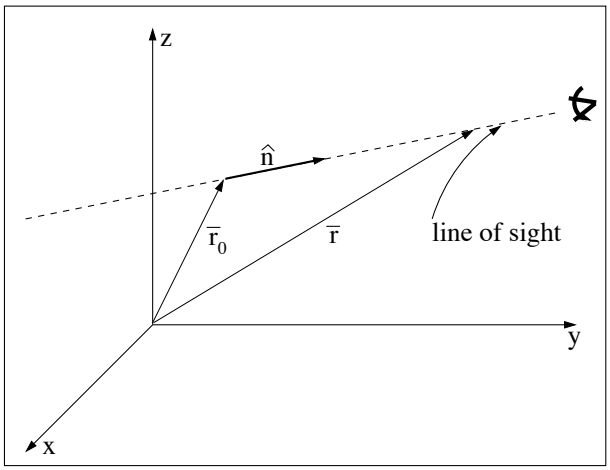

Fig. 3. Geometry of the calculations described in the text.

4. FARADAY ROTATION THROUGH A MAGNETIC DIPOLE FIELD

In order to illustrate the Faraday rotation produced by an object permeated by a non-uniform magnetic field, we study the case of a dipole magnetic field configuration. This dipole field could represent, e.g., the dipolar component of a multipolar expansion of a magnetic field with an arbitrary configuration. In order to obtain an analytic solution we furthermore assume that the object has a uniform density distribution for the ionized gas.

For a uniform density medium, the rotation measure (RM) is given by:

$$RM \equiv \int n B_\parallel ds = n I_B \,, \tag{1}$$

where

$$I_B \equiv \int B_\parallel ds \,, \tag{2}$$

is the integral along the line of sight of the component of the magnetic field along this line and n is the electron density. The line of sight is defined by its direction $\hat{n}$ and by a vector $\overline{r}_0$ which points to an arbitrary point of the line of sight (as shown in the schematic diagram of Figure 3). The vector $\overline{r}$ defining the path of the line of sight can then be written as:

$$\overline{r} = \overline{r}_0 + s\,\hat{n} \,, \tag{3}$$

where s is the distance along the line of sight to the point $\overline{r}_0$ and $\hat{n}$ is the unit vector along the line of sight (see Figure 3).

Let

$$\overline{r}_0 = x_0\,\hat{i} + y_0\,\hat{j} + z_0\,\hat{k}\,, \quad (4)$$
$$\hat{n} = n_x\,\hat{i} + n_y\,\hat{j} + n_z\,\hat{k}\,, \quad (5)$$

where $\hat{i}$, $\hat{j}$ and $\hat{k}$ are the unit vectors along the x, y and z axes, x_0, y_0 and z_0 are the coordinates defined by the $\overline{r}_0$ vector, and n_x, n_y and n_z are the components of the $\hat{n}$ unit vector. In spherical coordinates, the components of this unit vector can be written in the standard way as:

$$n_x = \sin\theta_0 \cos\phi_0\,, \quad (6)$$
$$n_y = \sin\theta_0 \sin\phi_0\,, \quad (7)$$
$$n_z = \cos\theta_0\,, \quad (8)$$

where θ_0 is the angle between $\hat{n}$ and the z-axis, and ϕ_0 is the angle between the xy-projection of $\hat{n}$ and the x-axis.

Then, the coordinates of an arbitrary point along the line of sight can be written as:

$$x = x_0 + s\,n_x\,;\;\; y = y_0 + s\,n_y\,;\;\; z = z_0 + s\,n_z\,. \quad (9)$$

In spherical coordinates, the (cylindrically symmetric) dipole field is:

$$\overline{B} = B_r\,\hat{r} + B_\theta\,\hat{\theta}\,, \quad (10)$$

where B_r is the component along the $\hat{r}$ direction of the spherical radius, $\hat{r}$ is the unit vector along $\overline{r}$ and B_θ is the component along the $\hat{\theta}$ direction of increasing angles with respect to the z-axis. The two components of the field can be written in the "far field approximation" (see, e.g., the book of Jackson 1975) as:

$$B_r = 2m\frac{\cos\theta}{r^3}\,;\;\; B_\theta = m\frac{\sin\theta}{r^3}\,, \quad (11)$$

where r is the spherical radius and m is the magnetic moment of the dipole.

Using the appropriate transformations between the (r,θ,ϕ) and (x,y,z) coordinates, one can write Equations (10-11) as:

$$\overline{B} = \frac{m}{r^5}\left[3xz\,\hat{i} + 3yz\,\hat{j} + (3z^2 - r^2)\hat{k}\right]\,, \quad (12)$$

with $r = \sqrt{x^2+y^2+z^2}$. This equation gives the dipolar magnetic field $\overline{B}$ (in the far field approximation) for an arbitrary point $\overline{r} = (x,y,z)$.

We now use Equations (9) and (12) to calculate the component $B_\parallel = \overline{B}\cdot\hat{n}$:

$$B_\parallel = m\big[n_x x_0(n_y s + 3z_0) + n_y y_0(n_z s + 3z_0) + \\ + n_x^2 s(2n_y s + 3z_0) + n_y^2 s(2n_z s + 3z_0) + \\ + n_z(2n_z^2 s^2 - x_0^2 - y_0^2 + 4n_z s z_0 + 2z_0^2)\big]\times \\ \times\left[(x_0 + n_x s)^2 + (y_0 + n_y s)^2 + (z_0 + n_z s)^2\right]^{-5/2}\,. \quad (13)$$

This value of $B_\parallel$ can now be integrated along the line of sight in order to obtain the rotation measure (see Equations 1-2).

Due to the cylindrical symmetry of the dipolar field, without any loss of generality we can consider lines of sight with $\phi_0 = 0$ (see Equations 7-8). We now also consider a coordinate system (x',y',z') in which the y' axis coincides with the y axis (see Figure 3), and with the x'- and z'-axes rotated (around the y-axis) at an angle θ_0, so that the x'-axis coincides with the line of sight. The $y'z'$ plane therefore coincides with the plane of the sky. The transformation between the (x,y,z) and (x',y',z') systems then is:

$$x = x'\sin\theta_0 - z'\cos\theta_0\,, \quad (14)$$
$$z = x'\cos\theta_0 + z'\sin\theta_0\,, \quad (15)$$
$$y = y'.$$

Combining equations (15-16) with Equation (13), we obtain:

$$B_\parallel = m\,\frac{(2s^2 - {y'_0}^2 - {z'_0}^2)\cos\theta_0 + 3sz'_0\sin\theta_0}{(s^2 + {y'_0}^2 + {z'_0}^2)^{5/2}}\,, \quad (16)$$

where $s = x'$ is the distance measured along the line of sight and (y'_0, z'_0) is the position of the line of sight on the plane of the sky.

Now, if we have a uniform, spherical density distribution with a finite volume, the rotation measure is determined by the I_B integral (see Equation 2), which, using Equation (16), gives:

$$I_B = \int_{s_1}^{s_2} B_\parallel ds = \\ m\left[\frac{s_1\cos\theta_0 + z'_0\sin\theta_0}{r_1^3} - \frac{s_2\cos\theta_0 + z'_0\sin\theta_0}{r_2^3}\right]\,, \quad (17)$$

where s_1 and s_2 are the points at which the line of sight crosses the outer edge of the emitting region, and $r_{1,2} = \sqrt{s_{1,2}^2 + {y'_0}^2 + {z'_0}^2}$ are the spherical radii of these two intercepts.

For the case of a spherical density distribution with an outer radius r_1, we have $s_2 = -s_1 = \sqrt{r_1^2 - {y'_0}^2 - {z'_0}^2}$, and Equation (17) takes the form:

$$I_B = -m \frac{2\cos\theta_0 \sqrt{r_1^2 - {y'_0}^2 - {z'_0}^2}}{r_1^3} \,. \qquad (18)$$

Notably, this result implies that once θ_0 is determined, the rotation measure (which is proportional to I_B, see Equation 1) only depends on the distance $\sqrt{{y'_0}^2 + {z'_0}^2}$ from the center of the (spherical) density distribution on the plane of the sky. Also, the value of the rotation measure decreases approximately as the inverse of the square r_1^2 of the outer radius for density distributions of larger radial extent. This result is true also for lines of sight that cross the central, high B, regions of the dipolar magnetic field. This can be seen by considering a line of sight crossing the center of the density distribution (i.e., with $y'_0 = z'_0 = 0$), and assuming that the far field approximation is still valid, for which from Equation (18) one obtains $I_B = 2m\cos\theta_0 / r_1^2$.

This result illustrates the fact that for extended objects with specific magnetic field distributions (in our case, a dipolar configuration), the rotation measure can have low values even while the magnetic field has high values in some of the regions of the object.

5. AN ESTIMATE OF THE MAGNETIC FIELD

In order to obtain an estimate of the magnitude of the magnetic field from our dipole model, we proceed as follows. From the map of Figure 1, we obtain $r_1 = 115'' = 0.27$ pc for the outer radius of the nebula, and a distance $b = \sqrt{{x'_0}^2 + {y'_0}^2} = 85'' = 0.20$ pc from the center of the nebula to the point at which we obtain the rotation measure (at a distance of 495 pc for the object).

Now, from Rodríguez et al. (2012), we have the relation:

$$I_B = 0.31 \left(\frac{RM}{10\,\mathrm{rad\,m^{-2}}}\right) \left(\frac{40\,\mathrm{cm^{-3}}}{n}\right) \mu\mathrm{G\,pc}\,. \qquad (19)$$

The modulus of the magnetic field is obtained from Equation (11):

$$B = \sqrt{B_r^2 + B_\theta^2} = \frac{|m|}{r^3}\sqrt{3\cos^2\theta_0 + 1}\,. \qquad (20)$$

Combining this equation with Equations (18) and (19) we then obtain:

$$B = 0.17\,\mu\mathrm{G} \left(\frac{|RM|}{0.4\,\mathrm{rad\,m^{-2}}}\right) \left(\frac{40\,\mathrm{cm^{-3}}}{n}\right) \left(\frac{0.20\,\mathrm{pc}}{r}\right)^3 \times \frac{1}{2}\sqrt{3 + \frac{1}{\cos^2\theta_0}}\,, \qquad (21)$$

we have used the values of r_1 and b given above, and left the dependencies on RM and n. From Equation (21), we see that:

- the dependence on the orientation angle is relatively weak, with the last term on the right hand side of Equation (21) having a value between 1 and 3 for angles between $\theta_0 = 0°$ to 80°,
- for the $RM \approx 0.4$ rad m^{-2} rotation measure and $n \approx 40$ cm^{-3} density values estimated for NGC 246, the magnetic field at a radius of 0.2 pc (equal to the projected distance at which we are obtaining the rotation measure) has a value between 0.17 μG and 0.51 μG, as long as θ_0 does not exceed 80°. The magnetic field will be correspondingly larger if θ_0 exceeds this value.

Clearly, because of the r^{-3} dependence (see Equation 21), our dipole model predicts substantially larger magnetic fields. As the ionized shell of the planetary nebula has an inner radius which is probably not smaller than ≈ 0.1 times its outer radius, our model would predict a magnetic field larger by at most a factor of $\approx 10^3$ (i.e., $B \approx 100\,\mu$G) at the inner edge of the shell.

6. CONCLUSIONS

We present JVLA observations made in the 1.3 to 1.8 GHz range toward the background extragalactic source J0047−1150, whose line of sight goes through the galactic planetary nebula NGC 246. We set a 4-σ upper limit to the rotation measure of 9.6 rad m^{-2} for J0047−1150.

This implies an upper limit to the average line-of-sight component of the magnetic field in NGC 246 of 1.3 μG. This is an extremely low value, although we argue that the local values of the magnetic field in the PN can be much larger. We show that the rotation measure for a line of sight across a dipolar magnetic field can be very small due to cancellation along the line of sight and that in this case we may not be able to detect the magnetic field using Faraday rotation. A model using a dipolar magnetic field

suggests that the true magnetic field in a planetary nebula can be orders of magnitude larger than the upper limits given by the Faraday rotation.

We thank the referee for valuable comments that improved the paper. LFR acknowledges the support of DGAPA, UNAM, and of CONACYT (México). AR and JC acknowledge support from the CONACYT grants 167611 and 167625 and the DGAPA-UNAM grants IA103315, IA103115, IG100516 and IN109715. This research has made use of the SIMBAD database, operated at CDS, Strasbourg, France.

REFERENCES

Bond, H. E., & Ciardullo, R. 1999, PASP, 111, 217
Burn, B. J. 1966, MNRAS, 133, 67
Condon, J. J., Cotton, W. D., Greisen, E. W., et al. 1998, AJ, 115, 1693
Costa, A. H., Spangler, S. R., Sink, J. R., Brown, S., & Mao, S. A. 2015, arXiv:1510.04664
Cox, D. P. 2005, ARA&A, 43, 337
Essey, W., Ando, S., & Kusenko, A. 2011, Astroparticle Physics, 35, 135
Farnes, J. S., Gaensler, B. M., & Carretti, E. 2014, ApJS, 212, 15
Fleck, R. C., Jr. 1983, ApJ, 264, 139
Harvey-Smith, L., Madsen, G. J., & Gaensler, B. M. 2011, ApJ, 736, 83
Heiles, C., & Chu, Y.-H. 1980, ApJ, 235, L105
Heiles, C., Chu, Y.-H., & Troland, T. H. 1981, ApJ, 247, L77
Hu, J. Y., Slijkhuis, S., Nguyen-Q-Rieu, & de Jong, T. 1993, A&A, 273, 185
Hua, C. T., Dopita, M. A., & Martinis, J. 1998, A&AS, 133, 361
Jackson, J. D. 1975, "Classical Electrodynamics" (New York: Wiley)
Jordan, S., Werner, K., & O'Toole, S. J. 2005, A&A, 432, 273
Leal-Ferreira, M. L., Vlemmings, W. H. T., Kemball, A., & Amiri, N. 2013, A&A, 554, A134
Miranda, L. F., Gómez, Y., Anglada, G., & Torrelles, J. M. 2001, Nature, 414, 284
Muthu, C., Anandarao, B. G., & Pottasch, S. R. 2000, A&A, 355, 1098
Perley, R. A., & Butler, B. J. 2013, ApJS, 206, 16
Purcell, C. R., Gaensler, B. M., Sun, X. H., et al. 2015, ApJ, 804, 22
Qiao, H.-H., Walsh, A. J., Gómez, J. F., et al. 2016, ApJ, 817, 37
Ransom, R. R., Kothes, R., Wolleben, M., & Landecker, T. L. 2010a, ApJ, 724, 946
Ransom, R. R., Kothes, R., Landecker, T. L., & Wolleben, A. M. 2010b, The Dynamic Interstellar Medium: A Celebration of the Canadian Galactic Plane Survey, 438, 268
Ransom, R. R., Kothes, R., Geisbuesch, J., Reich, W., & Landecker, T. L. 2015, ApJ, 799, 198
Roberts, D. A., Goss, W. M., van Gorkom, J. H., & Leahy, J. P. 1991, ApJ, 366, L15
Rodríguez, L. F., Gómez, Y., & Tafoya, D. 2012, MNRAS, 420, 279
Sabin, L., Zhang, Q., Zijlstra, A. A., et al. 2014, MNRAS, 438, 1794
Saikia, D. J., & Salter, C. J. 1988, ARA&A, 26, 93
Steffen, M., Hubrig, S., Todt, H., et al. 2014, A&A, 570, A88
Taylor, A. R., Stil, J. M., & Sunstrum, C. 2009, ApJ, 702, 1230
Thum, C., & Morris, D. 1999, A&A, 344, 923
Tiengo, A., Esposito, P., Mereghetti, S., et al. 2013, Nature, 500, 312
Trigilio, C., Umana, G., & Cohen, R. J. 1998, MNRAS, 297, 497
Troland, T. H., & Heiles, C. 1977, ApJ, 214, 703
Vallee, J. P. 1980, A&A, 86, 251
Vlemmings, W. H. T., & van Langevelde, H. J. 2008, A&A, 488, 619

Jorge Cantó: Instituto de Astronomía, UNAM, Apdo. Postal 70-264, 04510, México City, México.
Carlos Carrasco-González and Luis F. Rodríguez: Instituto de Radioastronomía y Astrofísica, Universidad Nacional Autónoma de México, Apartado Postal 3–72, 58090 Morelia, Michoacán, México.
Alice Pasetto: Max-Planck Institut für Radioastronomie (MPIfR), Auf dem Hügel 69, 53121 Bonn, Germany.
Alejandro C. Raga: Instituto de Ciencias Nucleares, UNAM, Ap. 70-543, 04510, México City, México.
Daniel Tafoya: Department of Earth and Space Sciences, Chalmers University of Technology, Onsala Space Observatory, 439 92 Onsala, Sweden.